16th Australasian Fluid Mechanics Conference
Crown Plaza, Gold Coast, Australia
2-7 December 2007

Aero-acoustic oscillations inside large deep cavities

M. El Hassan[1] **L. Labraga and L. Keirsbulck**

[1]Laboratoire de mécanique et d'énergetique
université de Valenciennes, Le mont Houy, Valenciennes 59300, France

Abstract

This investigation focuses on the pressure amplitude response, within two deep cavities characterized by their length over depth ratios (L/H = 0.2 and 0.41), under varying free stream velocity in a large wind tunnel. Experiments have shown that for deep rectangular cavities at low Mach number, oscillations of discrete frequencies can be produced. These oscillations appear when the free stream velocity becomes higher than a minimum value. In addition, as flow velocity is increased, upward jumps in oscillation frequency are observed in the two cavity configurations. Convection velocity of instabilities along the shear layer was measured using velocity cross-correlations. This study shows that the hydrodynamic modes of the cavity shear layer are correctly predicted by the Rossiter model when the convection velocity is determined and the empirical time delay is neglected. For L/H = 0.2 the first oscillation mode is observed on the spectrogram. For L/H = 0.41, both the first and the second mode have approximately the same amplitude. Time-resolved Particle image velocimetry measurements were performed to obtain the vorticity distribution during the oscillation cycle along the cavity shear layer. It is found that the number of structures in the cavity shear layer depends on the mode order of cavity oscillation.

Introduction

Turbulent flows over rectangular cavity may lead to an aeroacoustic coupling between the cavity shear layer oscillations and the acoustic modes of the installation. This aspect is studied in this paper for particularly deep cavity case (L/H = 0.2 and 0.41) which exhibits low frequency oscillations. This cavity configuration is encountered in many industrial processes, ranging from windows and sunroofs in automobiles and over pantograph in train vehicles. The characterization of the pressure oscillations inside and around cavity has been treated by many authors (Rossiter[1], Tam and Block[2], Rockwell and Knisely[3], Rockwell et al.[4] and others).

Cavity turbulent flow is characterized by a convection of instabilities in the cavity shear layer from the leading to the trailing corner of the cavity. In most cavity flows, turbulent boundary layer (TBL) separation is followed by a roll-up leading to coherent structures into the cavity shear layer. The number of these shear layer vortical structures depends on the TBL thickness (δ_0) and the cavity length (L). The coherent structures of the shear layer impinges on the downstream edge of the cavity, generating acoustical disturbances. Rossiter model [1] was used in most of the publications concerning this phenomenon. In this model, the determination of peak frequency, where high distinguished amplitude occurs, is important in quantifying pressure variations inside and around the cavity. This frequency depends on the mode order, cavity length and the convection velocity (u_c) of coherent structures in the shear layer. Moreover, the number of structures in the cavity shear layer depends on the mode order of cavity oscillation (Gharib and Roshko[5], Forestier et al.[6]). The flow visualization done by Gharib and Roshko[5] shows that for mode 2 of the oscillation, two wavelengths (or vortical structures) exist along the shear layer of the cavity, while in mode 3 there are three waves (or vortical structures). In our study, $5 < L/\theta_0 < 24$ and as will be seen, only the first Rossiter mode is present for $L/H = 0.2$. For $L/H = 0.41$, mode 1 and mode 2 are detectable.

Each cavity configuration is a complex subject and needs to be deeply studied. Indeed, many geometrical parameters influence the aerodynamic and the aero-acoustic behaviors around the cavity. Sarohia[7] determined the minimum cavity length for the onset of oscillations. The determination of this minimum length will depend on the flow parameters U_0 (free stream velocity), δ_0 (thickness of the TBL just upstream from the cavity), and ν (kinematic viscosity of fluid). Rockwell and Knisely[3] showed that the variation of the cavity length leads to multiple peaks in the pressure spectra. Knisely and Rockwell[8] varied the cavity length for constant U_0. They found that there is a slight change in amplitude of the component at the fundamental frequency (oscillation mode).

Schachenmann and Rockwell[9] found that the self-sustained oscillations of the cavity are strongly influenced by the acoustic modes of the pipe (no-flow resonant acoustic modes). A "locking-on" effect is observed around the acoustic modes and the variation of oscillation frequency tends to parallel that of the pipe mode frequency as the cavity length increases.

For shallow cavities, the flow exhibits strong three-dimensionality. The choice of small L/H values leads to a two-dimensional organization of the flow (Forestier et al. [6]). Therefore, two geometrical aspect ratio ($L/H = 0.2$ and 0.41) are studied in this paper.

The present research improves our knowledge in cavity oscillations phenomenon. New aspects could be summarized as followed.

1. The convection velocity was considered in most of previous studies as an empirical parameter ($u_c/U_0 = 0.57$ as proposed by Rossiter, where U_0 being the free stream velocity). In the present study, the convection velocity of structures was experimentally obtained from velocity cross-correlations. Convection velocity distribution of structures along cavity shear layer is discussed for both cavity configurations and for different freestream velocities.

2. The incoming turbulent boundary layer (TBL) characteristics affect the amplitude of events as was shown numerically by Gloerfelt et al.[10], and experimentally by Grace et al.[11] and Camussi et al.[12]. The long and large test section of the present investigation lead to a fully developed turbulent boundary layer characterized by a large thickness (δ_0). Boundary layer thickness of the present study $90 < \delta_0 < 210mm$ is greater than those of all previous studies concerning cavity oscillation phenomenon.

3. East[13] found that for small working section dimensions, the tunnel and the cavity interacted acoustically. However, with greater test section dimensions, no interference was discerned. This phenomenon was predicted as highly

probable in many previous studies. It is motivating our option of large test section dimensions.

4. Although the L/H = 0.41 configuration was previously studied at M = 0.8 (Forestier et al.[6] and Larchevequeet al.[14]), different flow conditions of the present study aims at accomplishing data related to this cavity configuration. Indeed, in the present study Mach numbers are very low and the flow regime is low-subsonic. On the other hand, convection velocity of structures was measured with different freestream velocities in the present work and exhibits a quite different behaviour between oscillating and non-oscillating regimes.

5. Particularly deep cavity (L/H = 0.2) is being studied. El Hassan et al.[15] has founded that this cavity configuration has different quantitative influence on the skin friction comparing with square cavity cases. The present study aims at showing how this particular deep cavity could affect shear layer oscillations.

Apparatus and experimental procedures

Wind tunnel and cavity model details

The experimental measurements have been conducted in the closed circuit low speed wind tunnel of the Mechanics and Energetic Laboratory of Valenciennes. The test section is $2 \times 2\ m^2$ in cross-section and 10 m long. The maximum outlet velocity along the centerline of the test section is 60 m/s. The relative turbulence level at 30 m/s is about 0.5%. Measurements were made at free stream stream velocities covering the range 1 to 56 m/s. The dimensions of the first cavity configuration were L = 104 mm in length, H = 520 mm in depth and W = 2000 mm in width. Aspect ratios were L/H = 0.2 and L/W = 0.052. The second cavity configuration had the same H and W as the first one, with L = 213 mm. Its ratios were L/H = 0.41 and L/W = 0.107. Three-dimensional view of cavity is shown in Figure 1. Each cavity was installed on the lateral wall of the test section, with the leading edge located 8 m downstream from the test section inlet. The boundary layer was characterized just upstream of the cavity leading edge. Hot-wire measurements of velocity profiles at this location showed that for low velocity ($U_0 = 2m/s$) the boundary layer was fully developed. These measurements, at low free stream velocities, show that the boundary layer thickness (δ_0 = 18 cm) corresponds to that found in a fully developed boundary layer.

Pressure measurements

Kulite pressure transducers were employed, with a nominal sensitivity of 275 mv/bar. The outputs from the transducers were connected to a multi-channel signal conditioner. Data acquisition of pressure signals is accomplished using an A/D board with $12 - bit$ resolution. A gain adjustment was used in order to meet the required voltage input levels of the A/D board. Data were sampled at 6 kHz typically for 180000 samples (30 $sec.$) from each channel. The acquired pressure signals were low-pass filtered with a cut-off frequency of 3 kHz, to avoid aliasing effects. Wall pressure measurements were made by using 3 flush-mounted Kulite sensors. The sensitive region of the probes is a small circle 2.5 mm in diameter. One sensor ($PS1$) was set on the leading edge at y = -30 mm. The second sensor ($PS2$) was positioned at the cavity bottom at x = 80 mm and 130 mm for $L/H = 0.2$ and 0.41 respectively. The third sensor ($PS3$) was located on the trailing edge at y = -30 mm. Locations of sensors are indicated in Figure 2.

Figure 3 shows two pressure spectrums obtained for $U_0 = 46m/s$. This figure confirms that for the two cavity configurations no interesting physical features exist in the present flow at high frequencies. Oscillating modes and their harmonics are detected at low frequencies. Therefore, F = 500 Hz will be the maximum frequency of interest for all pressure analysis.

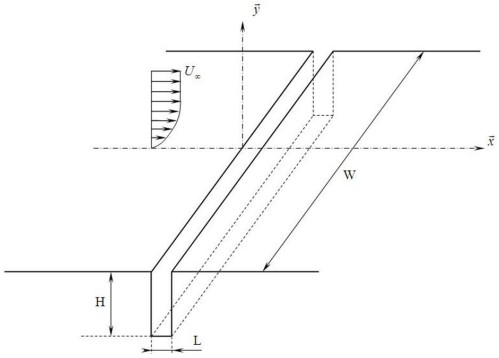

Figure 1: three-dimensional view of the cavity

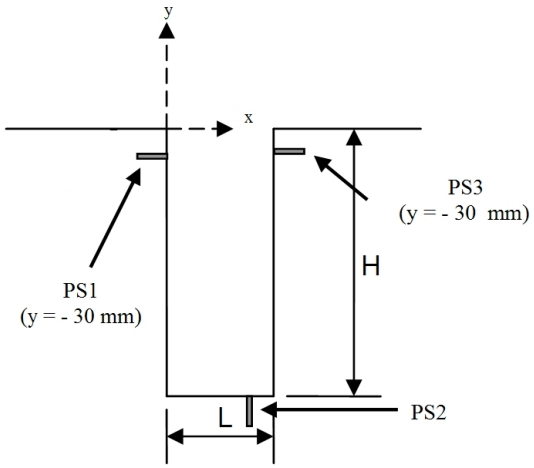

Figure 2: Kulite sensors positions

Hot-wire measurements

Experiments were carried out using a DANTEC 55M10 constant temperature hot-wire anemometry (CTA) system. The output signal was transferred by an A/D digital card connected to a PC. The STREAMLINE software supplied by DANTEC was used to acquire and store data. A boundary layer type probe was used for the boundary layer measurements upstream from the cavity. Two single wire probes DANTEC 55P15 were used for cross-correlation measurements in the cavity shear layer. The sensors of both probes consisted of platinum-tungsten wires. Streamwise time-space correlations between velocity signals were performed in order to calculate the convection velocity of structures. These cross-correlation measurements were obtained using two single hot-wire sensors placed in the shear layer at $y = 0$ close to the center in the spanwise direction. The space between the two probes was made using a manually controlled mechanism with an accuracy of 10 μm. The longitudinal space between the two hot-wires was then fixed to 8 mm. A small shift (about 1 mm) of the two hot-wire probes was performed in the spanwise direction in order to avoid a streamwise wake interaction between probes. The relative turbulent level (RTL) was measured along the shear layer for each freestream velocity. In all cases, RTL is inferior to 15 % rendering the adopted cross-correlation technique feasible. A traversing system was used to move the probes in the streamwise direction. A

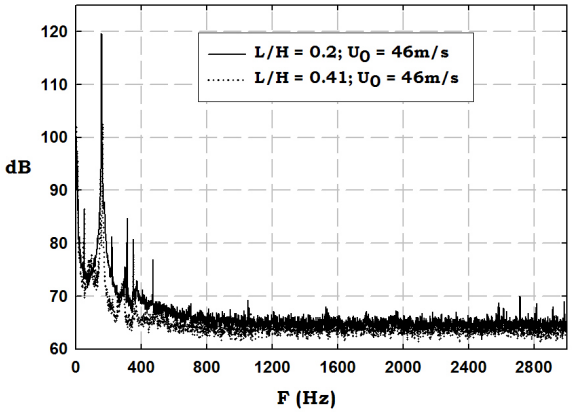

Figure 3: Pressure spectrum from PS4 (kulite sensor at the leading edge)

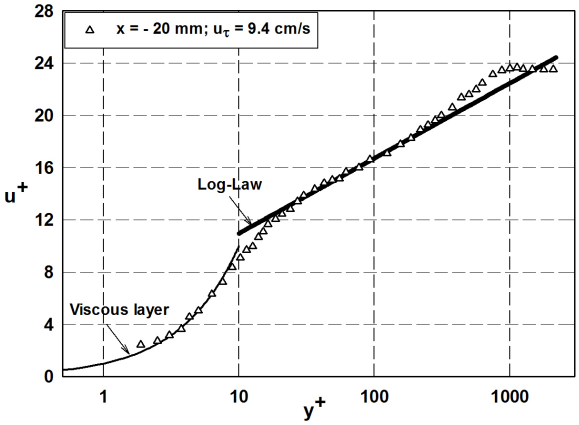

Figure 4: Mean streamwise velocity profile upstream of the cavity

traverse grid was defined for each cavity configuration. For each free stream velocity, data are acquired along the shear layer. The signals from the C.T.A. were filtered and amplified to give signals that covered most of the $\pm 10\,V$ range of the A/D converter.

Time resolved PIV measurements

The PIV system is based upon a time resolved PIV Dantec 'DynamicStudio' system, including a $2 \times 10mJ$ dual YAG laser, a 3 kHz Photron Ultima APX-RS Camera (1024 x 1024 pixels) used at 2 kHz frequency (1 kHz vector map). The time between two laser pulses used for the experiments presented here was $30\mu s$ for L/H = 0.2 and $50\mu s$ for L/H = 0.41. The PIV camera was mounted on a traversing system, perpendicular to the light sheet plane of the laser. PIV measurements were taken in a streamwise plane (x, y) normal to the wall. In order to keep the same resolution for L/H = 0.41 than that of L/H = 0.2 configuration, the field for L/H = 0.41 had to be divided into two subregions with an overlapping area (30 mm in the streamwise direction). These two regions were combined to investigate the whole length of the cavity. The overlapping area allowed the choice of upstream and downstream fields of the same flow phase and thus the time tracking of individual vortices.

Results

Incident turbulent boundary layer

Single hot-wire measurements were done 20 mm upstream from the cavity leading edge in order to lay down the characteristics of the incident boundary layer. Figures 4 and 5 respectively show the mean streamwise velocity profiles and its root-mean-square turbulent level for $U_0 = 2m/s$. These profiles illustrate the turbulent and fully developed aspect of the incident boundary layer. The low sub-sonic velocity (2 m/s) allows measurements in the viscous layer and hence accurate estimation of the skin friction velocity (u_τ). In the figure 4, u^+ and y^+ are normalized using u_τ. The log-law fits well the data for $30 < y^+ < 300$. Turbulent boundary layer parameters are deduced from velocity profile. At $U_0 = 2m/s$ the boundary layer upstream of the cavity had a shape factor $H = \delta_1/\theta_0 = 1.32$ where $\delta_1 = 22.5mm$ (displacement thickness), $\theta_0 = 17mm$ (momentum thickness) and $Re_{\theta_0} = 2267$.

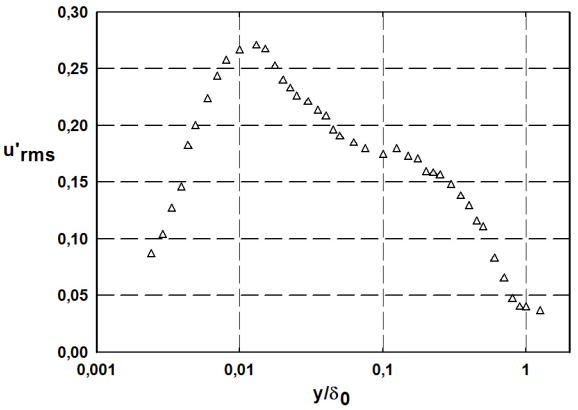

Figure 5: Streamwise root-mean-square profile upstream of the cavity

Structures advection along the shear layer

Figure 6 shows three cross-corrrelation plots obtained at three different spacements (e = 4, 6 and 8) between hot-wire probes. These plots have particular peaks at relatively high amplitude. This result reflects a high level of interdependence between informations obtained from the two single hot-wires. Peaks occur with a time delay T^+ which represents the time for structures to travel from the first to the second hot-wire in the streamwise direction.

The two single hot-wire sensors positions were along the constante $y = 0$ line of the shear layer. This y position was chosen considering that in shear-layer mode, the vortical structures travels in the streamwise direction along the cavity shear layer and are detected by the first then the second hot-wire sensor. Although the trajectory of the vortical structures could be influenced by the acoustic waves, Gloerfelt et al.[17] asserters that well-aligned vortices are presents in the cavity shear layer with a slight growth of vortices when approaching the downstream corner of the cavity. Moreover, Rowley et al.[16] noted that the interaction of the flow inside the cavity with the shear layer is relatively weak. Preliminary measurements were made with different espacements (e) between the two hot-wires. Similar distributions (not shown in this paper) of the convection velocity for e = 4, 6, 8 and 11 mm were obtained. This allowed us to choose a fixed space (e = 8 mm) for all the measurements of the convection velocity along the shear layer for both cavity configurations.

Structures or instability waves present in the cavity shear layer

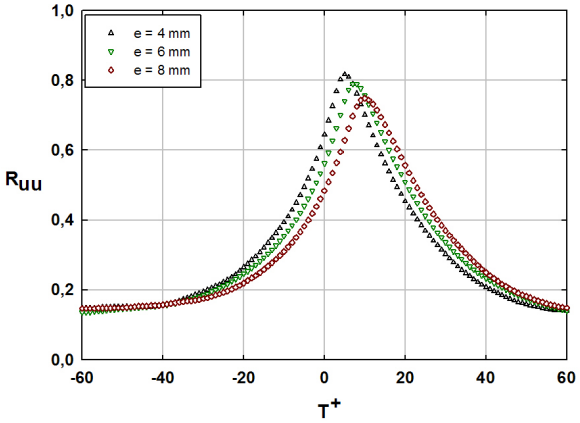

Figure 6: Velocity cross-correlation obtained from two single hot-wire placed in the cavity shear layer

are convected from the leading to the trailing edge of the cavity with a characteristic convection velocity $u_c = e/T^+$. The ratio u_c/U_0 of the Rossiter formula was often considered by authors as empirical and taken as a constant value along the shear layer (Kegerise and Spina[18]; Hirahara et al.[19]). Our results prove that the convection velocity of eddies depends on the position of the structures over the mixing layer. In the empirical formula found by Rossiter, u_c/U_0 was 0.57. Rossiter has proposed the equation:

$$S_t = \frac{fL}{U} = \frac{n-\alpha}{M+\frac{1}{\kappa}} \quad (1)$$

where n is the cavity mode, κ is the ratio of the convection velocity of structure to the free stream velocity, and α the lag time between the impact of a structure on the cavity downstream corner and the emission of an acoustic wave. This parameter was always taken as empirical value and is adjusted to fit experimental data (as done by Rossiter). At moderate Mach number there is an acoustic delay $\alpha = 0.25$ (Rowley et al.[16]).

Figures 7 and 8 show the distribution of the convection velocity, normalized by the free stream velocity, plotted against x/L with x being the longitudinal position of the structures along the mixing layer.

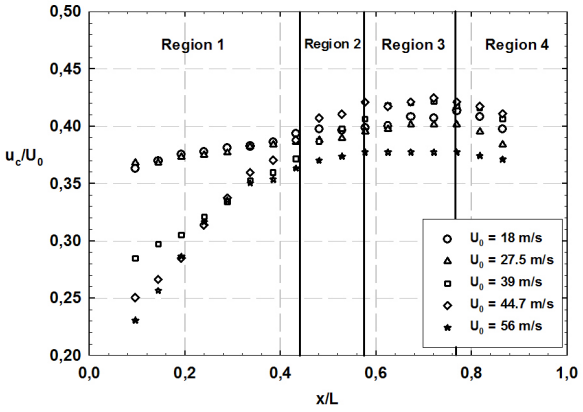

Figure 7: Convection velocity distribution along cavity shear layer ($L/H = 0.2$)

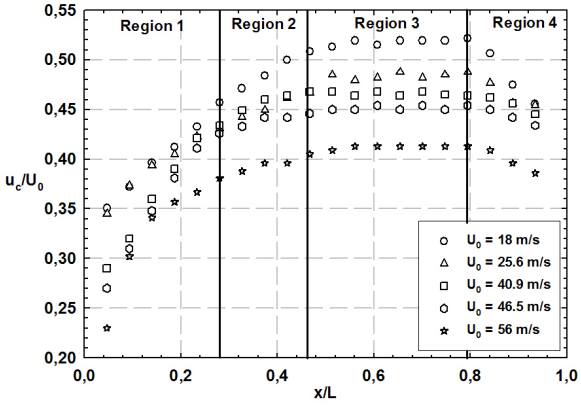

Figure 8: Convection velocity distribution along cavity shear layer ($L/H = 0.41$)

In all cases, the detachment of the turbulent boundary layer at the cavity leading edge is followed by an acceleration of the structure in the mixing layer. Four regions could be distinguished (figures 7 and 8)

1. Region1: coherent structure acceleration is constant and is more pronounced for higher free stream velocities.
2. Region2: characterized by an acceleration of the structures slower than in region1.
3. Region3: u_c remains almost constant. The corresponding plateau is larger in $L/H = 0.41$ compared to $L/H = 0.2$.
4. Region4: the structures decelerate and the convection velocity decreases.

In order to calculate the oscillating frequency of the shear layer, the u_c values corresponding to $x/L = 0$ and $x/L = 1$ was estimated by extrapolation of plots.

Figures 7 and 8 show a quite different behavior with respect to shear layer oscillations. Indeed, in zone 1 and for L/H = 0.2, structures acceleration is lower in non-oscillating case. This could be explained by an important instability amplifications near to the cavity leading edge due to acoustic feedback process and consequently an important (acceleration of structures).

The convection time scale (T_c) taken by structures to cross the cavity length was calculated by integrating the convection velocity along the shear layer as shown in Eqn 4.

$$T_c = \int_0^L \frac{dx}{u_c(x)} \quad (2)$$

Therefore, a mean convection velocity was obtained as the ratio of the cavity length to the time (T_c). The convection velocity obtained for each free stream velocity was used with the Rossiter formula for both $\alpha = 0$ and $\alpha = 0.25$. This was applied to mode 1 and mode 2 of cavity oscillations. Accurate determination of peak frequencies from spectrum analysis allowed calculation of Strouhal numbers $St = f \times L/U_0$. Results are shown in figures 9 and 10. These plots show that the results obtained from Rossiter formula with $\alpha = 0$ fit in with the emergences of various modes. Indeed, this value of $\alpha = 0$ adequately predicts the modes of the cavity oscillation in both cavity configurations of

the present study. While for $\alpha = 0.25$, plots diverge from emergences and never cross them. Rossiter[1] has suggested that α decreases with L/H. Moreover, Larchevêque et al.[14] proposed that the extension of the Rossiter model to the deep cavity accurately predicts the peak frequency when α is adjusted. From their measurements, these authors found that agreement is achieved for $\alpha = 0.038$. The main difference between the two studies is Mach number value which was of 0.8 while in the present study it is less than 0.17. Chatellier[20] suggested that at low Mach numbers, the retroaction due to the interaction of the shear layer and the impingement corner is instantaneous and considers that the related parameter (α) should be negligible. This hypothesis leads to a correct application of the Rossiter formula on his results when adjusting κ. In conclusion, when Mach number is low and for deep cavity configuration, α seems to be very close to zero. Finally, the good prediction of oscillation frequencies by the Rossiter formula, confirms the existence of a feed-back process leading to global instability.

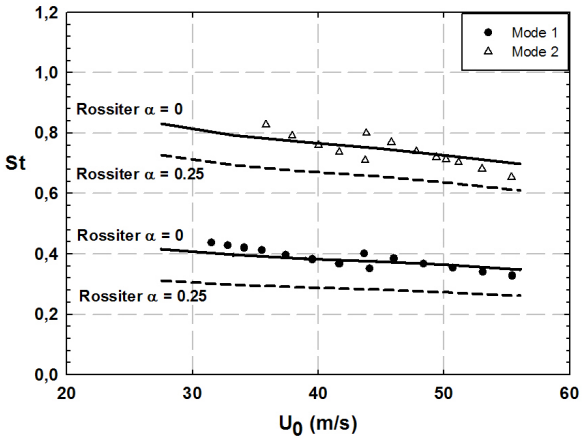

Figure 9: Strouhal number of oscillating frequencies for L/H = 0.2, solid symbols: strongest mode, solid lines: Rossiter modes using measured u_c and $\alpha = 0$, dashed lines: Rossiter modes using measured u_c and $\alpha = 0.25$

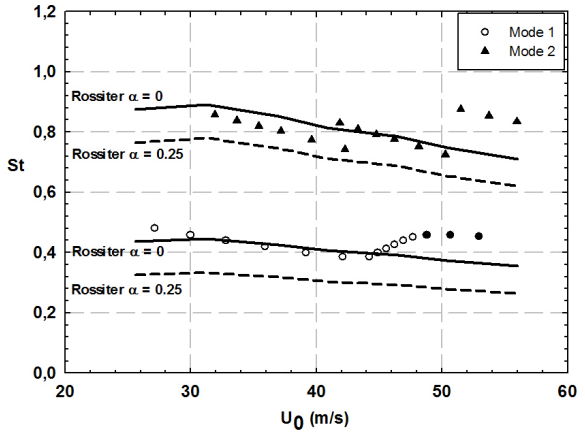

Figure 10: Strouhal number of oscillating frequencies for L/H = 0.41, solid symbols: strongest mode, solid lines: Rossiter modes using measured u_c and $\alpha = 0$, dashed lines: Rossiter modes using measured u_c and $\alpha = 0.25$

Vortical structures along the cavity shear layer

Q-factor vortex identification criterion has been employed. This criterion was proposed by Hunt et al.[21]:

$$Q = \frac{1}{2}(\Omega_{ij}\Omega_{ij} - S_{ij}S_{ij}) \tag{3}$$

where Ω_{ij} and S_{ij} are the anti-symmetrical and symmetrical part of the tensor gradient of velocity :

$$\Omega_{ij} = \frac{1}{2}(\frac{\partial u_i}{\partial x_j} - \frac{\partial u_j}{\partial x_i}) \tag{4}$$

$$S_{ij} = \frac{1}{2}(\frac{\partial u_i}{\partial x_j} + \frac{\partial u_j}{\partial x_i}) \tag{5}$$

The presence of coherent structures in the flow is evidenced on the Q-field obtained from two-components velocity field. The use of this method is motivated by the presence of high velocity gradients in the cavity shear layer flow.

For L/H = 0.2 and $U_0 = 43m/S$, two-dimensional instantaneous velocity and Q-factor fields of seven shear layer flow phases are plotted in figures 11, 12, 13, 14, 15, 16 and 17. These figures show a vortical structure (S) traveling from the leading to the trailing edge of the cavity.

1. Phase 1 : Following a roll-up of the incident boundary layer, a vortical structure S is formed just downstream the cavity leading edge. Flow ejection is present close to the downstream corner. This outflow process has begun at the last phase of previous cycle.

2. Phase 2 : The vortical structure has moved downstream along the shear layer. The ejection process is weaker near the downstream corner than it was in phase 1.

3. Phase 3 : S has grown. No exchange is discernible between inside the cavity and the outflow.

4. Phase 4 : S got bigger and is located equidistantly between the leading and the trailing edge.

5. Phase 5 : S occupies a major part of the shear layer just ahead of the cavity downstream corner.

6. Phase 6 : In the shear layer downstream part, S is oriented towards the corner with its greater part being inside the cavity.

7. Phase 7 : The major part of S has sunk along side the cavity downstream corner. A beginning of ejection process could be observed above this corner.

   In all phases, a big recirculation zone spanning the entire length of the cavity is observed in the upper part of this one. There's flow exchange between this recirculating zone and S. In addition, clusters of moderate-scale vorticity concentrations are clipped off and travel along the vertical surface of the trailing wall upper part.

Figure 18 illustrated the existence of two vortical structures with same rotational direction in the cavity shear layer for L/H = 0.41 and $U_0 = 37m/s$.

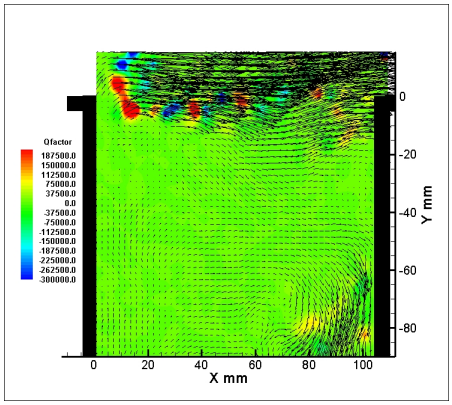

Figure 11: Phase 1 of cavity shear layer oscillating cycle (L/H = 0.2)

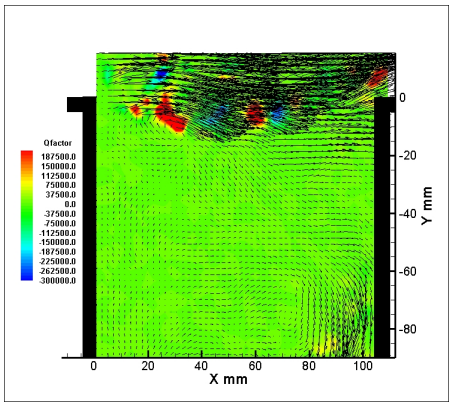

Figure 12: Phase 2 of cavity shear layer oscillating cycle (L/H = 0.2)

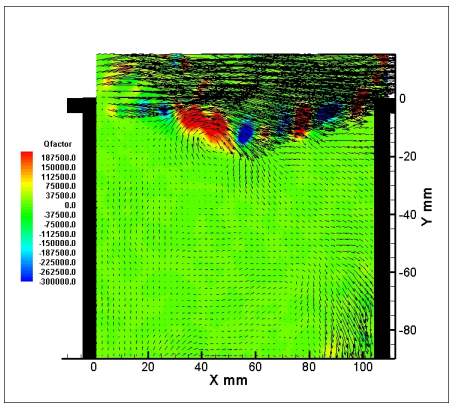

Figure 13: Phase 3 of cavity shear layer oscillating cycle (L/H = 0.2)

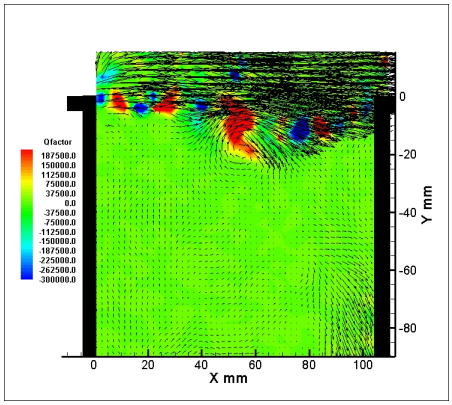

Figure 14: Phase 4 of cavity shear layer oscillating cycle (L/H = 0.2)

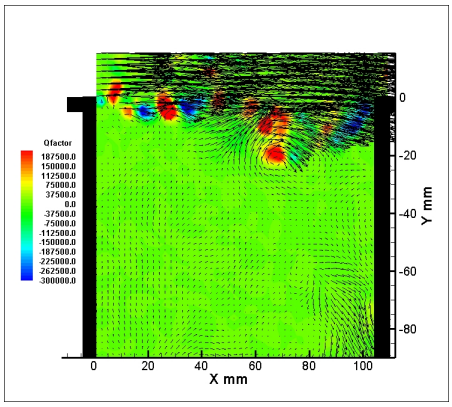

Figure 15: Phase 5 of cavity shear layer oscillating cycle (L/H = 0.2)

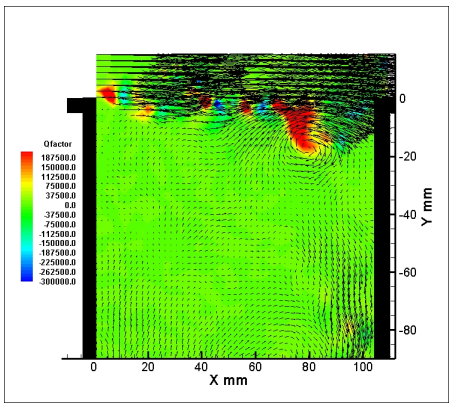

Figure 16: Phase 6 of cavity shear layer oscillating cycle (L/H = 0.2)

Conclusion

Experimental characterization of the inside pressure fluctuations at low Mach numbers has been conducted in two deep cavity models. Measurement of the convection velocity of structures, along the cavity shear layer, has been performed using hot-wire cross-correlation. The main conclusions could be summarized as followed.

(a) Instabilities in the shear layer are convected from the leading edge to the trailing edge of the cavity with a non constant convection speed (u_c). Four different regions are identified along the cavity shear layer. Behavior of u_c in the first region is quite different in so far as cavity mode oscillates or not. The higher acceleration of oscillating-regime is attributed to acoustic amplification of the shear layer instabilities in the upstream part of the cavity.

(b) Rossiter formula correctly predicts the hydrodynamic modes of deep cavities with a convection velocity which has been measured and with $\alpha = 0$. This implies that the generation of acoustic retroaction is instantaneous for low Mach numbers.

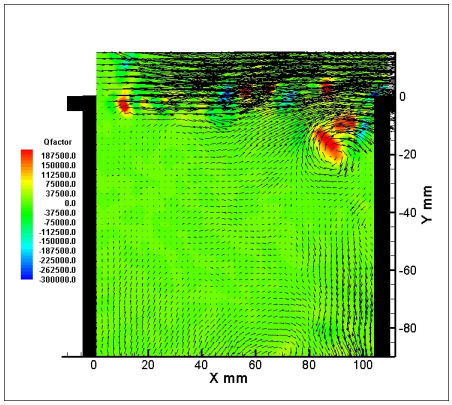

Figure 17: Phase 7 of cavity shear layer oscillating cycle (L/H = 0.2)

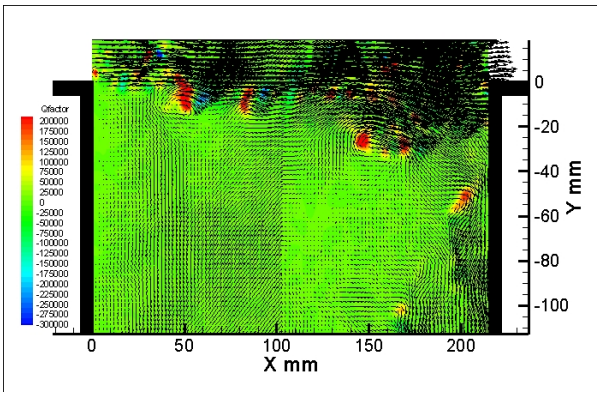

Figure 18: Phase of cavity shear layer oscillating cycle showing two vortical structures along the shear layer (L/H = 0.41)

(c) Strouhal number of cavity oscillations corresponds to the first cavity mode (Rossiter model) for L/H = 0.2 and to both the first and second cavity modes for L/H = 0.41. The pressure amplitudes show a stronger lock-in between hydrodynamic and acoustic modes for L/H = 0.2 than L/H = 0.41. This leads to a more significant maximum SPL in the first configuration.

(d) With an aspect ratio of L/H = 0.2, oscillations of the shear layer excit acoustic modes of the cavity, leading to a generation of flow tones. This aero-acoustic coupling is less obvious with L/H = 0.41. Although, as flow velocity is increased, upward jumps in oscillation frequency is observed in the two cavity configurations.

(e) The maximum SPL distributions at different locations on cavity walls highlighted the SPL maximum magnitude is reached at the cavity bottom and reveals a strong excitation of the depth mode by the shear layer oscillation at this location.

(f) For L/H = 0.2, shear layer oscillations begins at $L/\theta_0 \approx 10$ which is much lower than values found in previous studies. This difference is attributed to both the highly turbulence aspect of the incident boundary layer as well as the acoustic depth mode of the cavity.

(g) During an oscillating cycle, the shear layer rolls up into a number of vortical structures. It was found that the number of structures present in the cavity shear layer is equal to the highest mode order of cavity oscillation (1 for L/H = 0.2 and 2 for L/H = 0.41).

References

[1] Rossiter J.E., 1964, "Wind tunnel experiments on the flow over rectangular cavities at subsonic and transonic speeds, " Aeronautical Research Council Reports and Memo No. 3438

[2] TAM, C.K.W., and BLOCK, P.J.W., 1978, "On the tones and pressure oscillations induced by flow over rectangular cavities," J.Fluid Mech., **89**, No 2, pp. 373-399

[3] Rockwell, D., and Knisely, C., 1980, "Vortex-edge interactions: mechanism for generating low frequency components," Physics of fluids, **23**, No 2, pp. 239-240

[4] Rockwell, D., Lin J.-C., Oshkai, P., Reiss, M., and Pollack, M., 2003, "Shallow cavity flow tone experiments: onset of locked-on states," journal of fluids and structures, **17**, pp. 381-414

[5] Gharib, M., and Roshko A., 1987, "The effect of flow oscillations on cavity drag," Journal of Fluid Mechanics, **177**, pp. 501-530

[6] Forestier, N., Jacquin, L., and Geffroy, P., 2003, "The mixing layer over a deep cavity at high-subsonic speed," J. Fluid Mech., **475**, pp. 101-145

[7] Sarohia, V., 1975, "Experimental and analytical investigation of oscillations in flows over cavities," PhD Thesis, California Institute of Technology

[8] Knisely, C., and Rockwell, D., 1982, "Self-sustained low-frequency components in an impinging shear layer," J. Fluid Mech., **116**, pp. 157-186

[9] Schachenmann, A., and Rockwell, D., 1980, "Self-sustained oscillations of turbulent pipe flow terminated by an axisymmetric cavity," Journal of sound and vibration, **73**, Issue 1, pp. 61-72

[10] Gloerfelt, X., Bogey, C. and Bailly, C., 2003, "Numerical evidence of mode switching in the flow-induced oscillations by a cavity, International Journal of Aeroacoustics", **2:2**, pp. 193-217

[11] Grace, S.M., Dewar, W.G. and Wroblewski, D.E., 2004, "Experimental investigations of the flow characteristics within a shallow wall cavity for both laminar and turbulent upstream boundary layers", Experiments in Fluids, **36**, pp. 791-804

[12] Camussi, R., Guj, G., and Ragni A., 2006, "Wall pressure fluctuations induced by turbulent boundary layers over surface discontinuities," Journal of Sound and Vibration, **294**, Issues 1-2 pp. 177-204

[13] EAST, L. F., 1966, "Aerodynamically induced resonance in rectangular cavities," Journal of Sound and Vibration, **3**, Issue 3 pp. 277-287

[14] Larchevêque, L., Sagaut, P., Ivan, M., and Labbé O., 2003, "Large-eddy simulation of a compressible flow past a deep cavity," Physics of fluids, **15**, No 1 pp. 193-210

[15] El Hassan, M., Labraga, L., and Keirsbulck, L., 2007, "Écoulement turbulent affleurant une cavité profonde" 18ème Congrés Français de Mécanique

[16] Rowley, C.W., Colonius, T. and Basu, A.J., 2002, "On self-sustaining oscillations in two-dimensional compressible flow over rectangular cavities", J. Fluid Mech., **455**, pp. 315-346

[17] Gloerfelt, X., Bailly, C. and Juvé, D., 2003, "Direct computation of the noise radiated by a subsonic cavity flow and application of integral methods," J. Sound Vib., **266**, Issue 1, pp. 119-146.

[18] Kegerise, M. A., Spina, E. F., Garg, S., and Cattafesta, L. N., 2004, "Mode-Switching and Nonlinear Effects in Compressible Flow Over a Cavity," Physics of Fluids, **16**, No 3, pp. 678-687

[19] Hirahara, H., Kawahashi, M, Uddin Khan M., and Hourigan, K., 2007, "Experimental investigation of fluid dynamic instability in a transonic cavity flow," Experimental Thermal and Fluid Science, **31**, No 4, pp. 333-347

[20] Chatellier, L., 2002, "Modélisation et contrôle actif des instabilités aéroacoustiques en cavité sous écoulement affleurant," Université de Poitiers, thèse

[21] Hunt, J.C.R., Wray A.A., and Moin P., 1988, "Eddies, stream, and convergence zones in turbulent flows," Center for turbulence research Rep. CTR-S88

[22] Bergmann, D., Kaiser, U., and Wagner, S., 2003, "Reduction of low-frequency pressure fluctuations in wind tunnels," Journal of Wind Engineering and Industrial Aerodynamics, **91**, No 4, pp. 543-550

[23] Ricot, D., Maillard, V. and Bailly, C., 2002, "Numerical simulation of unsteady cavity flow using Lattice Boltzmann Method," **8th** AIAA/CEAS AeroAcoustics Conference, AIAA Paper, pp. 2002-2532

[24] Williams, J. F. 1992, "Modern Methods in Analytical Acoustics Lecture Notes," The Journal of the Acoustical Society of America, **92**, No 5, pp. 313-354